Fiber amplifiers and lasers

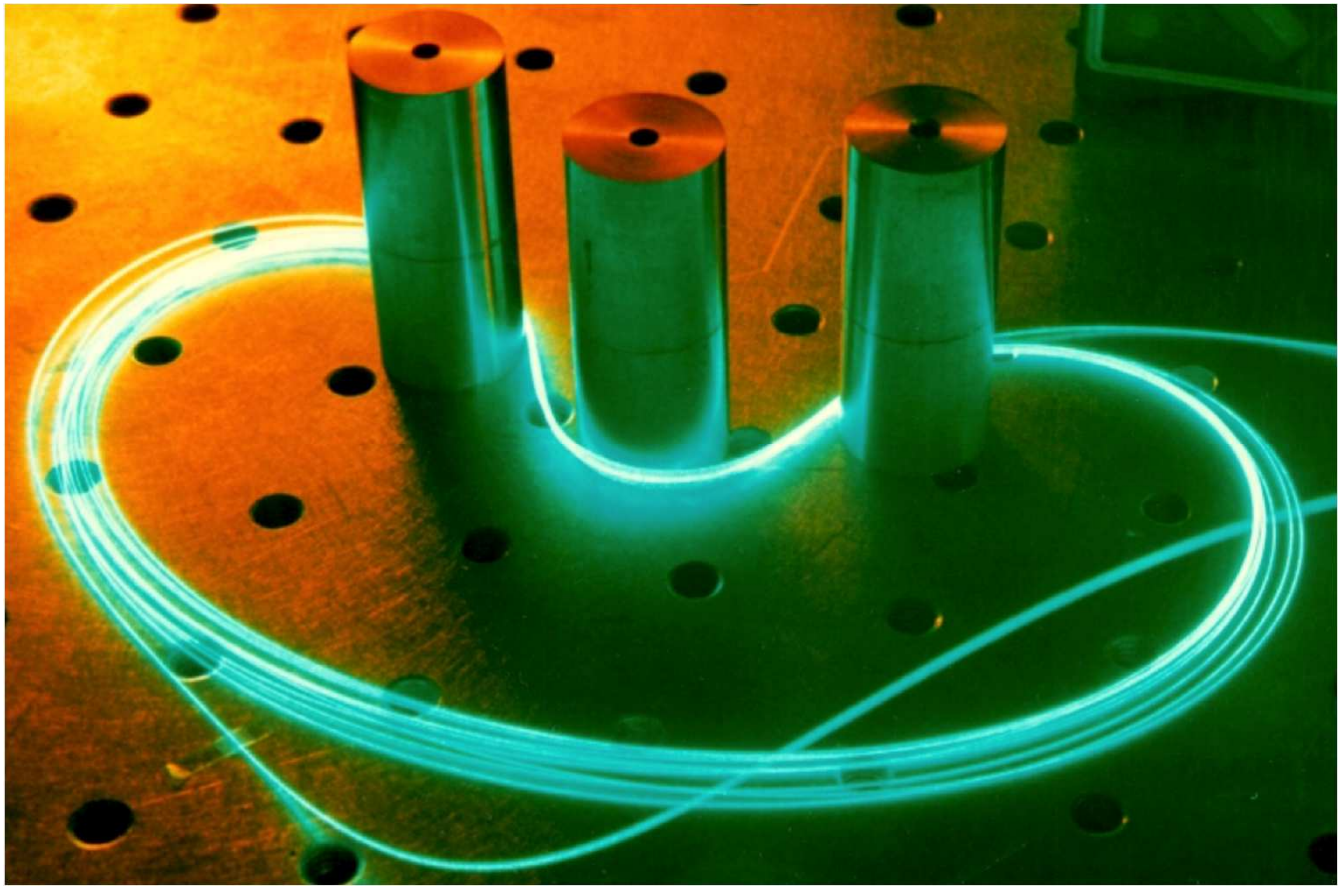

Prof. Sébastien Février

Fig. 1 (a) Periodic table. (b) Possible site for Er^{3+} in basic silicate glass.

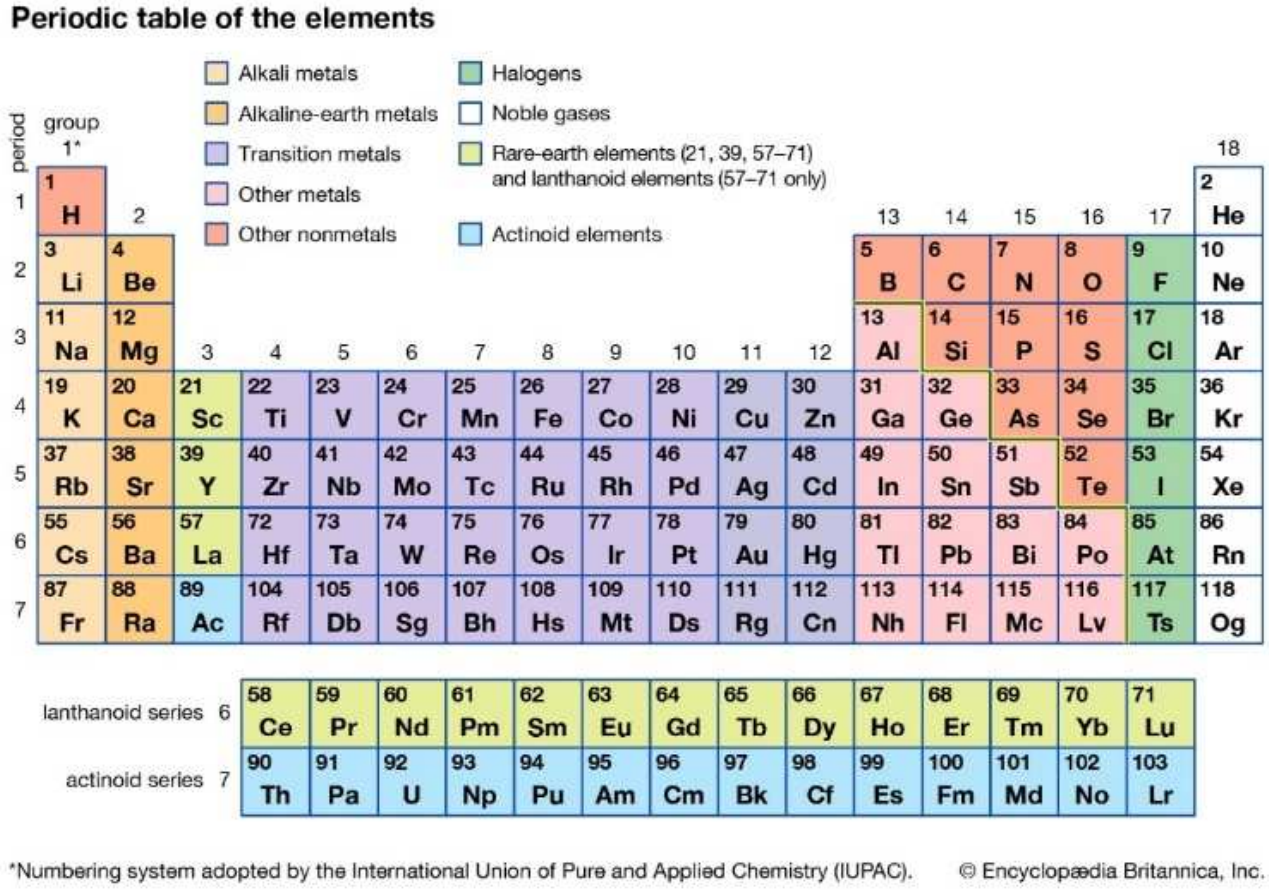

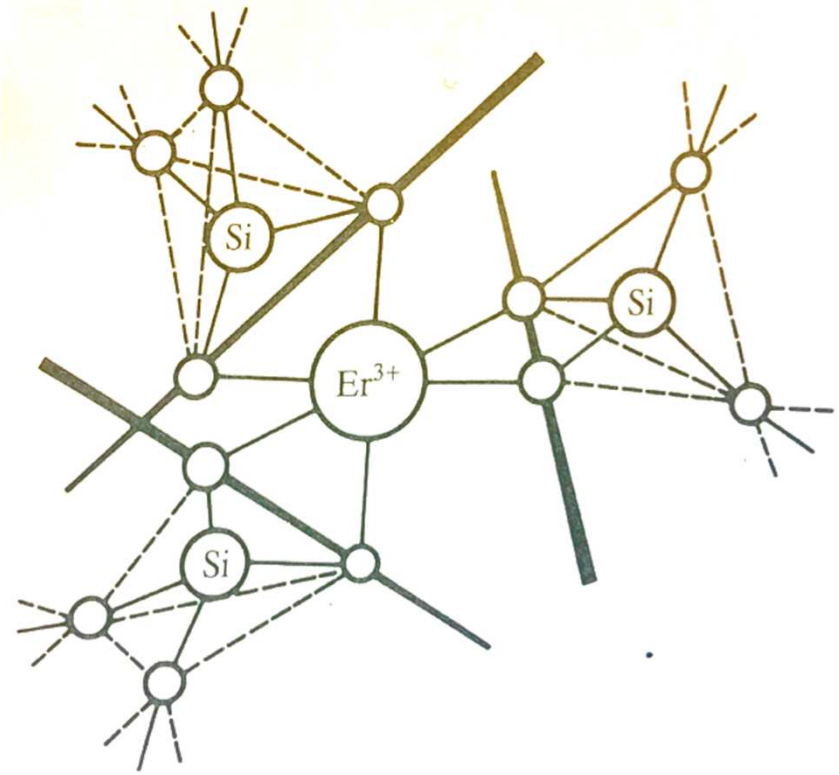

Fig. 2 (a) MCVD process for low vapor-pressure dopants from S. B. Poole and D. N. Payne, and M. E. Fermann "Fabrication of low-loss optical fibres containing rare-earth ions," in *Electronics Letters*, vol. 21, no. 17, pp. 737-738, 15 August 1985) **(b) Refractive index profile of a prefom fabricated b MCVD (c) Schematic of the fiber drawing tower**

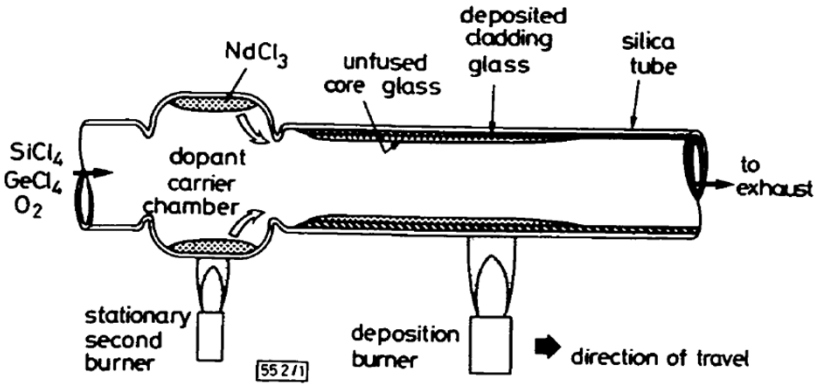

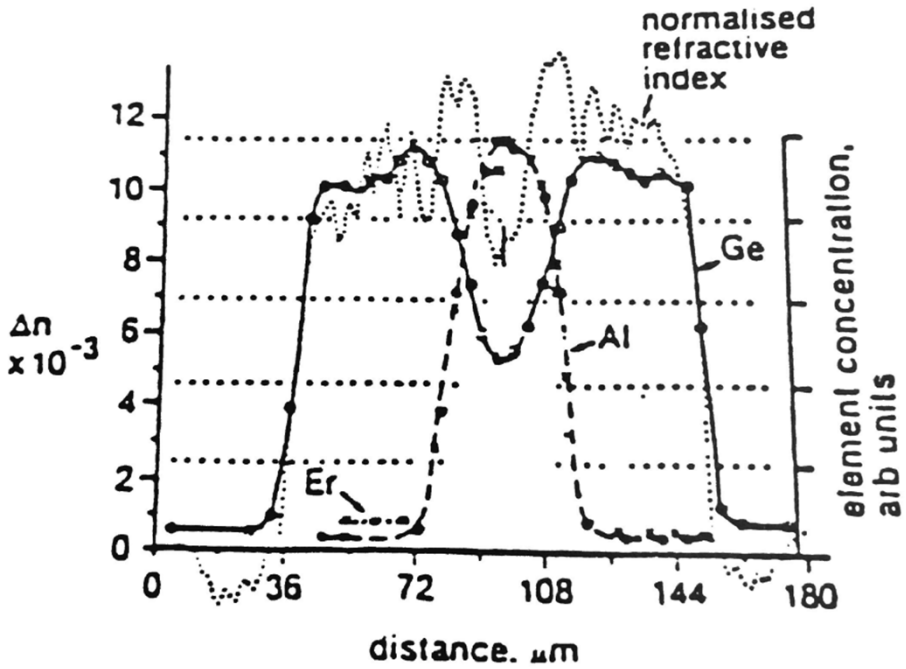

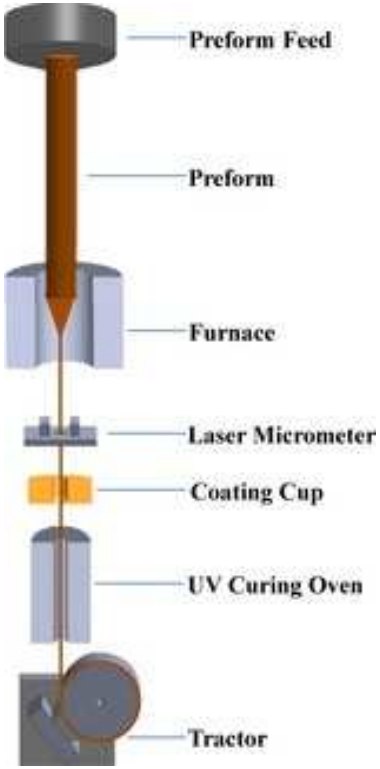

Prof. Sébastien Février

Fig.3 (a) Absorption spectrum of fiber containing 2 parts in 10^6 of Er^{3+} (from S. B. Poole and D. N. Payne, and M. E. Fermann "Fabrication of low-loss optical fibres containing rare-earth ions," in *Electronics Letters*, vol. 21, no. 17, pp. 737-738, 15 August 1985). **(b) Energy level diagram for Er^{3+}.**

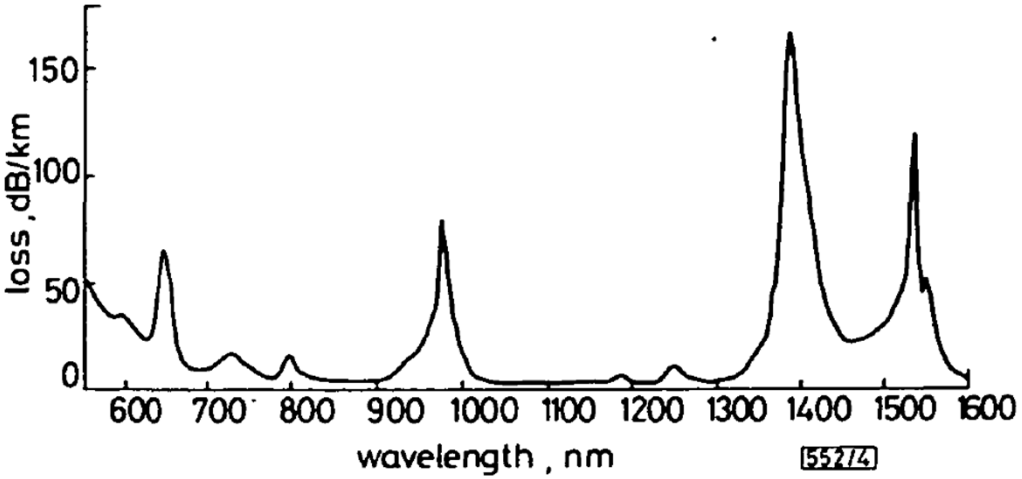

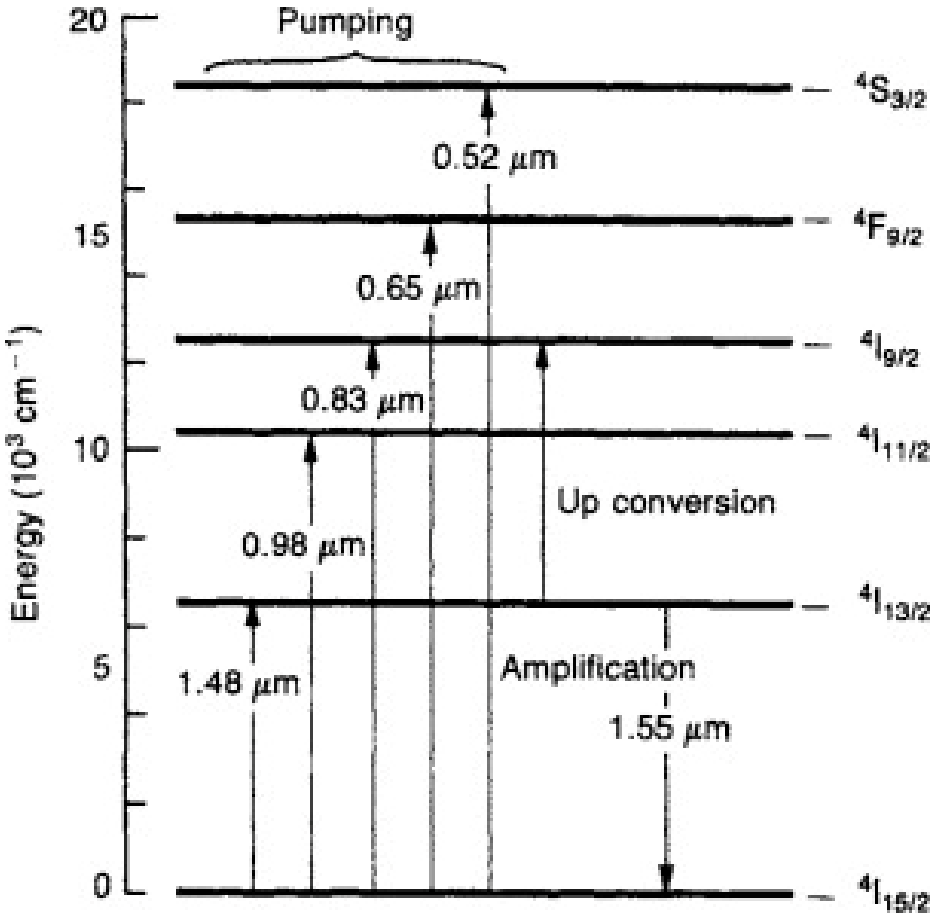

Prof. Sébastien Février

Fig. 4 (a) Absorption spectrum of fiber containing 30 parts of Nd^{3+} in 10^6 parts. (b) Fluorescence spectrum of fiber containing 300 parts of Nd^{3+} in 10^6 parts.

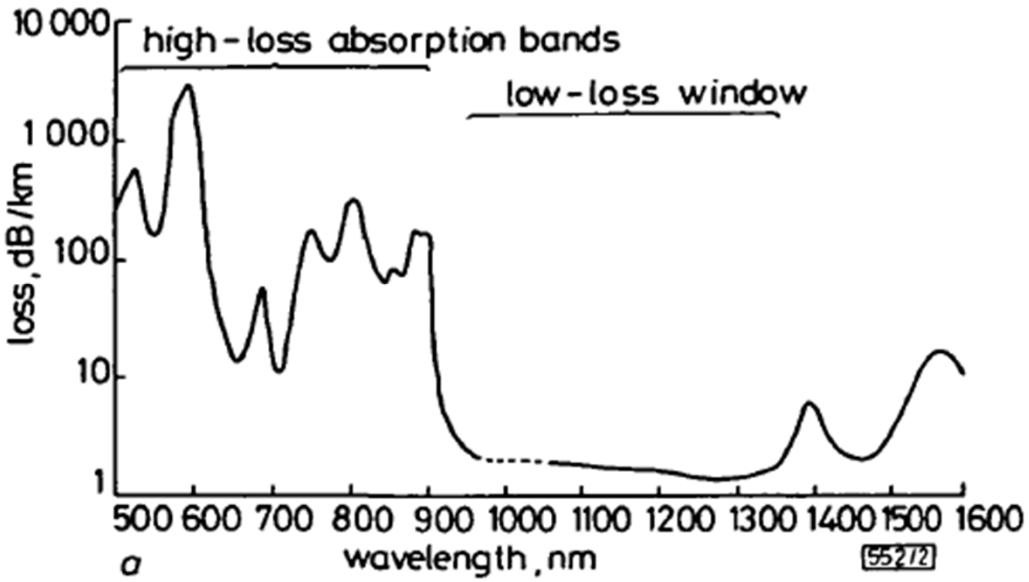

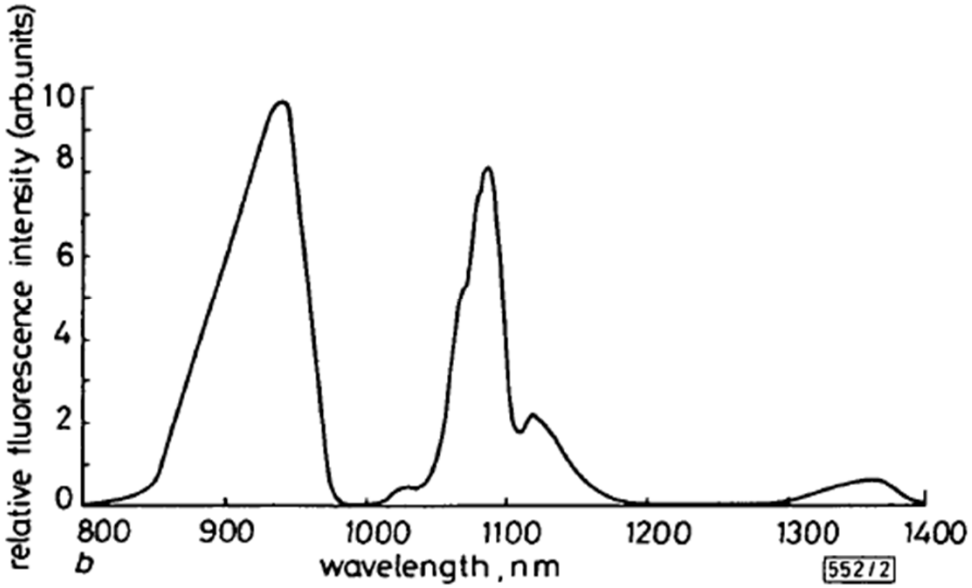

Fig. 5 The laser transitions for trivalent RE in glass hosts and corresponding energy levels.

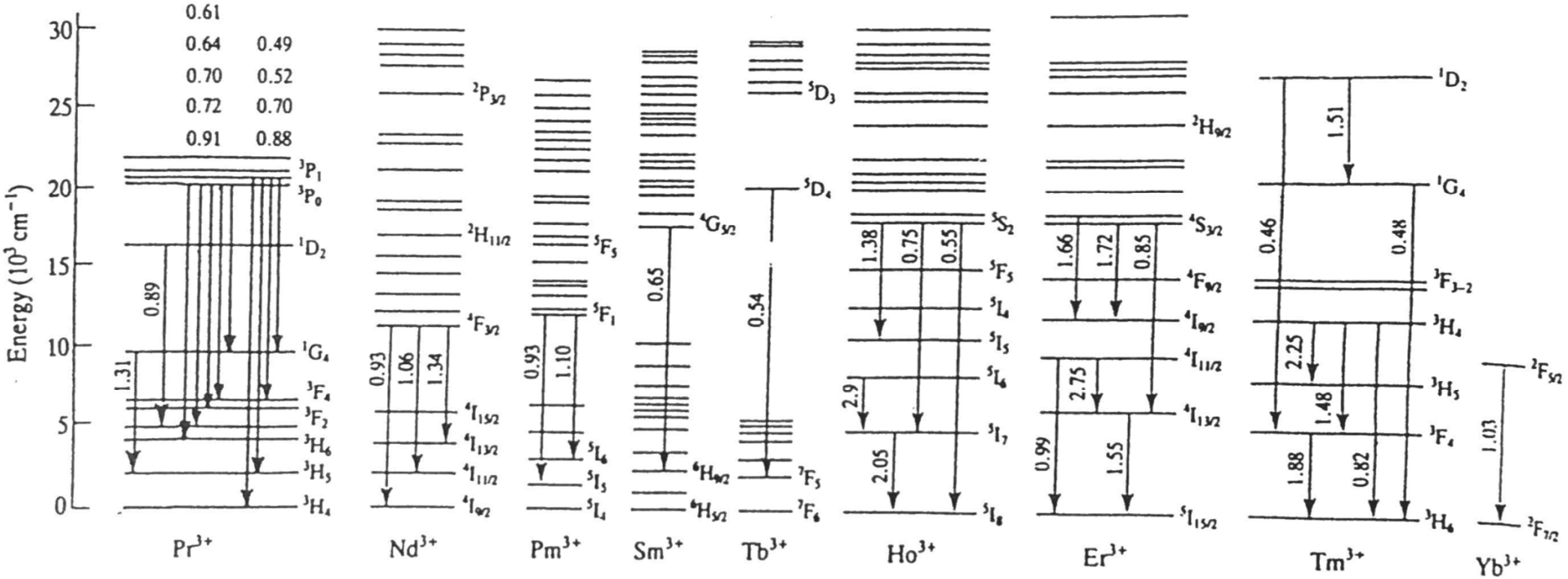

Fig. 6 Effect of Stark splitting of energy levels with degeneracies g_1 and g_2, caused by crystalline electric field E, with possible laser transitions.

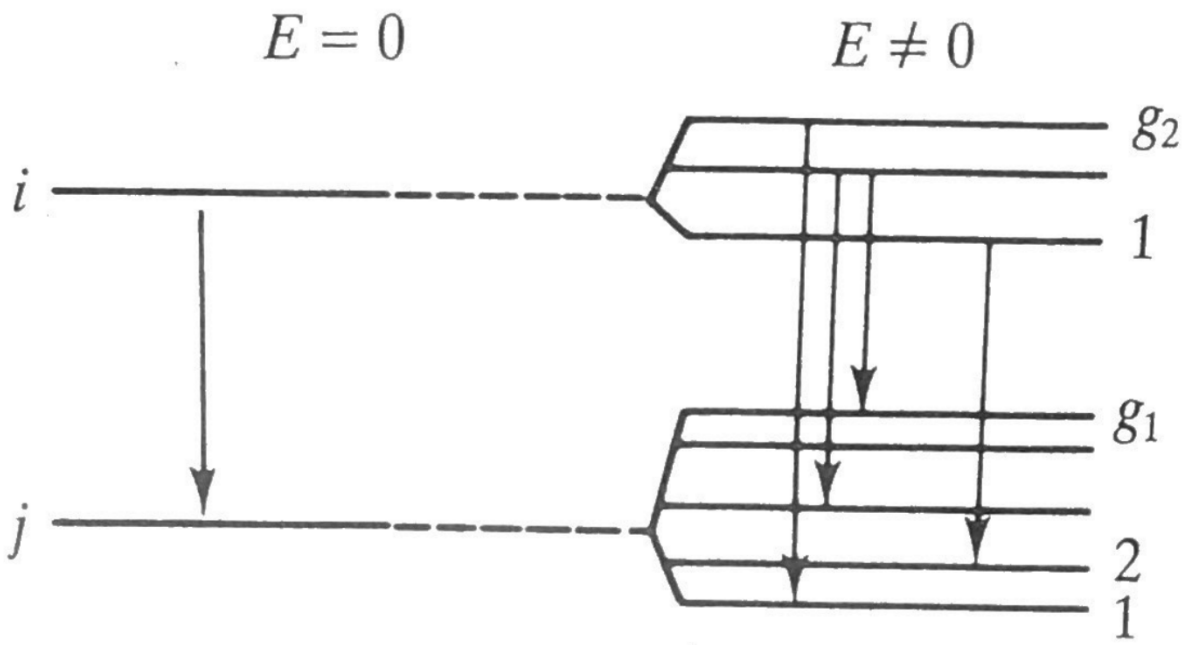

Prof. Sébastien Février

Fig. 7 Effect of inhomogeneous broadening, where random field variations from site to site cause changes in the Stark splitting and center wavelength of laser transitions.

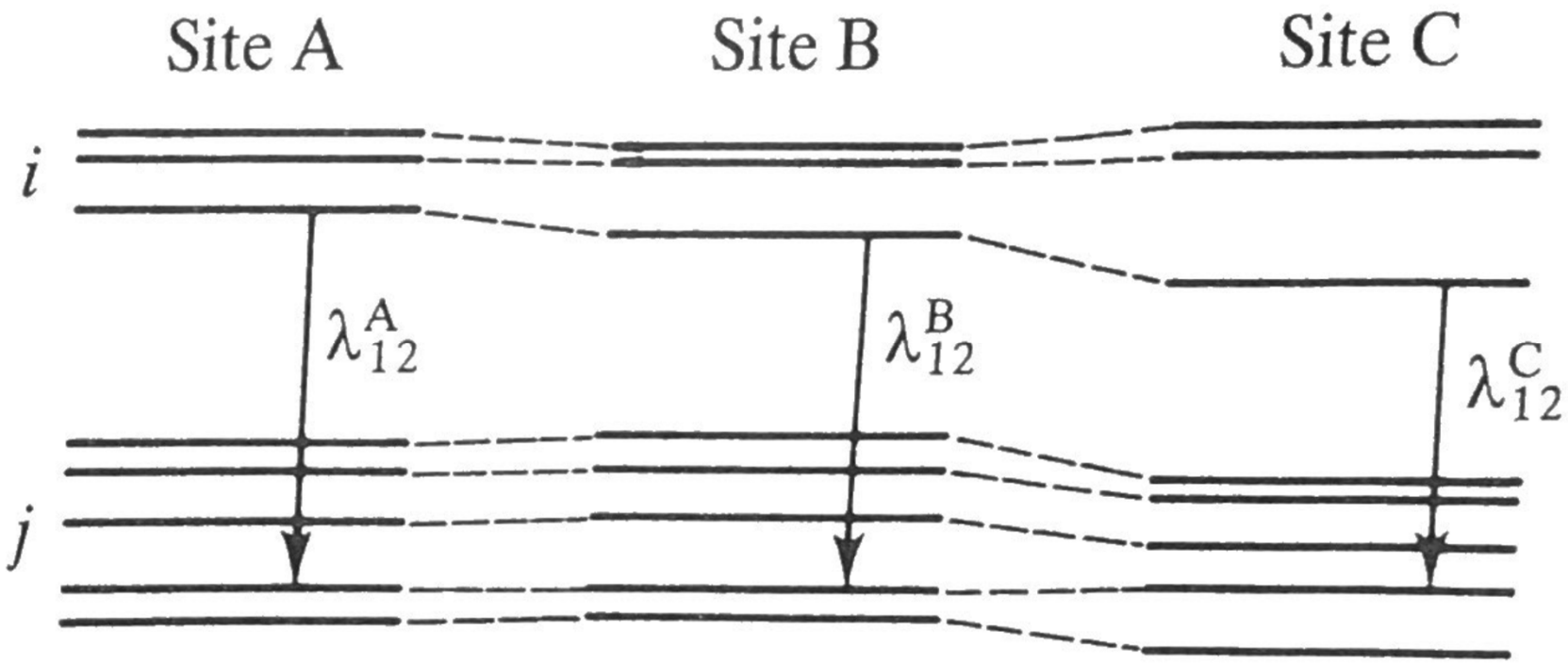

Fig. 8 (a) Absorption and fluorescence spectra of aluminosilicate Er-doped fiber showing structures changes and positions of Stark transitions. (b-c) Stark transitions corresponding to absorption and emission spectra shown in (a).

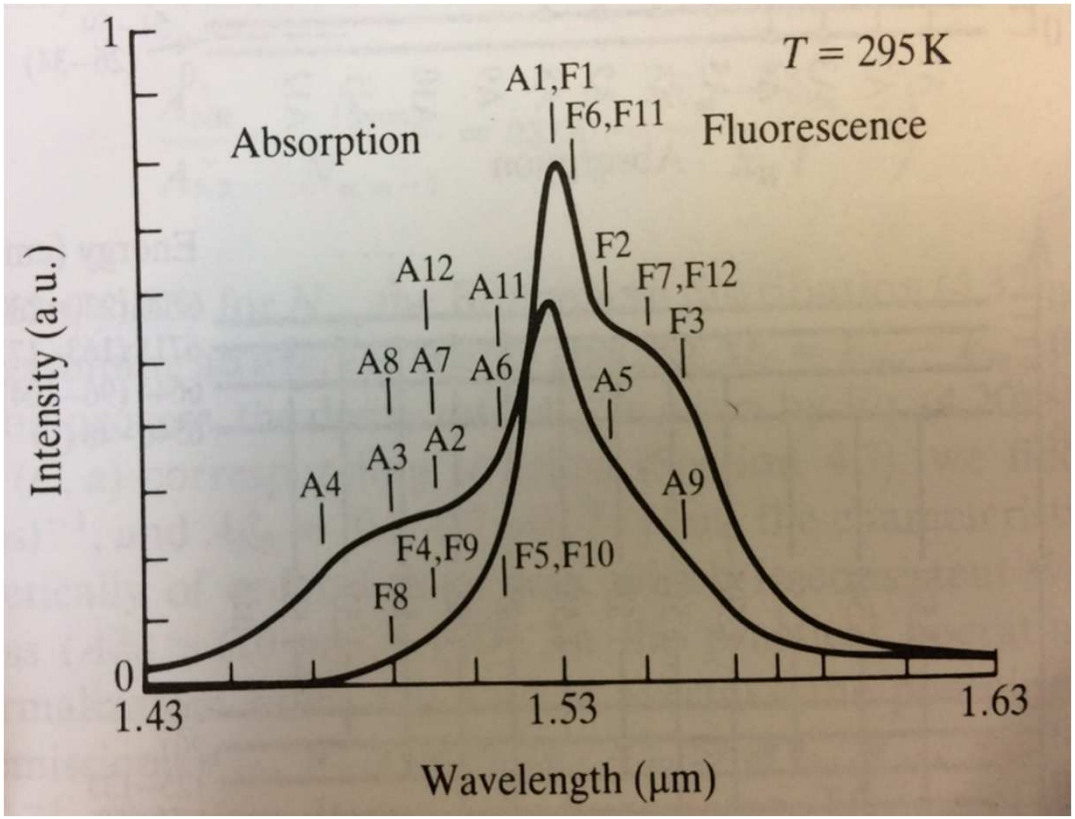

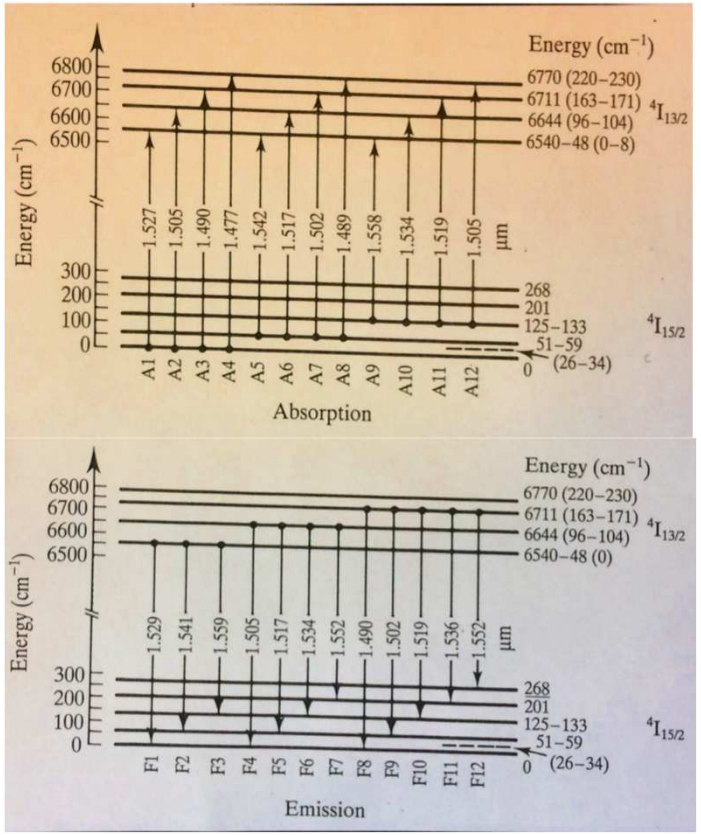

Prof. Sébastien Février

Prof. Sébastien Février